Electronic Supplementary Material (ESI) for Analyst.

Anomalous scattering of polystyrene microparticles by evanescent wave coupled cavity ring-down spectroscopy

Soumyadipta Chakraborty,[a] Jayeta Banerjee,[a] Indrayani Patra,[a] Ardhendu Pal,[a] Puspendu Barik*[,b] and Manik Pradhan*[,a]

[a]*Chemical and Biological Sciences, S. N. Bose National Centre for Basic Sciences, JD Block, Sector-III, Salt Lake City, Kolkata - 700106, India*
[b]*GPL Photonics Laboratory, State Key Laboratory of Applied Optics, Changchun Institute of Optics, Fine Mechanics and Physics, Chinese Academy of Sciences, Changchun, China*

*Corresponding author: pbarik_mid1983@yahoo.co.in, manik.pradhan@bose.res.in

Sample description

The approximate number of particles per ml (N) can be calculated from the equation:

$$N = \frac{6W \times 10^{12}}{\rho \pi d^3}$$

W = grams of polymer per ml in latex (0.1 g for a 10% solid sample)
d = diameter in microns of PSM particles (5 μm std dev <0.1 μm, coeff var <2%)
ρ = density of polymer in grams per ml (1.05 for polystyrene)

Table S1 The description of samples used in the experiments with different concentrations expressed by the volume fraction (φ), number density (N), refractive index (n)

Sample name	The volume fraction of PSM, φ ($\times 10^{-4}$)	Number density, N ($\times 10^6\ /ml$)	Refractive index, n	Zeta potential, ζ (mV)	Particles per unit area of sample surface from SEM images (/mm^2)
S01	0	0	1.33294	$-27.1 \pm 5.7\ mV$	
S02	1.75	2.67	1.33295		70
S03	1.93	2.95	1.33290		
S04	2.16	3.30	1.33287		
S05	2.45	3.74	1.33280		
S06	2.82	4.32	1.33283		
S07	3.34	5.10	1.33279		90
S08	4.08	6.24	1.33288		
S09	5.25	8.02	1.33287		
S10	7.35	11.23	1.33276		
S11	12.25	18.72	1.33272		134
S12	13.12	20.05	1.33278		
S13	14.14	21.59	1.33284		
S14	15.31	23.39	1.33273		
S15	16.70	25.52	1.33262		
S16	18.37	28.07	1.33281		430
S17	20.42	31.19	1.33231		
S18	22.97	35.09	1.33219		
S19	26.25	40.11	1.33208		633
S20	30.62	46.79	1.33229		710

Experimental setup and characterization of the EW-CRDS system

A stable, open and linear optical cavity of length, $L \sim 1.35\ m$ was established with two broadband highly reflective plano-concave mirrors (R > 99.98% for 400−800 nm, LAYERTEC GmbH, Radius of curvature = 1 m). The free spectral range ($\Delta\nu_{FSR}$) or the fundamental mode spacing is $\Delta\nu_{FSR} = c/2L = 1.11 \times 10^8\ Hz$. The high reflectivity of the cavity mirrors results a very high finesse of $F = (2R/1 - R^2)^2 = 2.5 \times 10^7$, exhibiting weak phase distortions. A diode laser (MDL-NS/AP-635-80mW, divergence $< 1.0\ mrad$, CNI

Optoelectronics Technology Co., Ltd.) was used as a continuous source. Fig. S1(a) shows 2D and 3D profiles of the laser, centre wavelength ($\lambda = 638.5\ nm$), line width ($\Delta\nu \sim 0.361 \times 10^{12}\ Hz$), or the full width at half maximum ($FWHM \sim 0.491\ nm$), fitting with the Gaussian peak profile. The broad line width of the laser can accommodate cavity modes $N = {}^{\Delta\nu}/_{\Delta\nu_{FSR}} = 3252$ within a single laser mode; hence, the cavity is always in resonance once aligned.

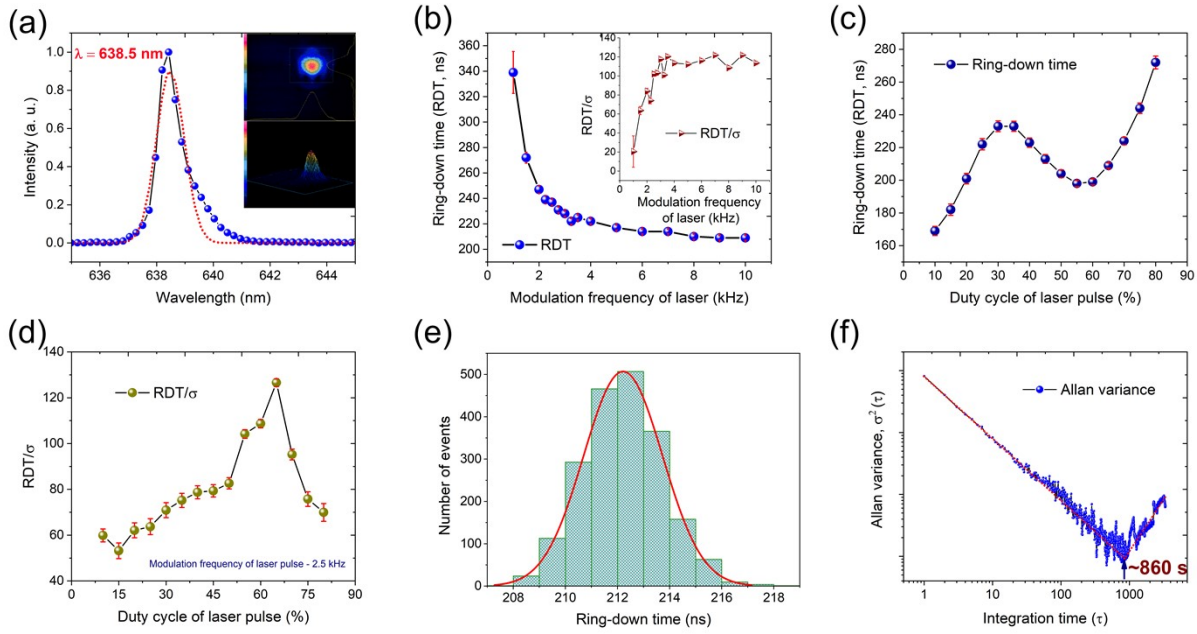

Fig. S1. *(a) The measured and Gaussian-fitted spectra show the laser's centre wavelength. The insets in the figure show the 2D and 3D profiles of the laser. (b) The variation of ring-down time (RDT) with the change in laser modulation frequency. The inset shows the variation of the ratio of RDT and standard deviation (σ) with the modulation frequency of the laser pulse. (c)The variation of RDT with duty cycle maintaining laser modulation frequency at 2.5 kHz (d) The variation of the ratio of RDT and standard deviation (σ) with duty cycle of laser pulse maintaining laser modulation frequency at 2.5 kHz. (e) Distribution of the baseline ring-down time fitted with a normal or Gaussian distribution. (f) Allan variance analysis of measurement stability.*

A pulse generator (TGP-110-*TTi*) was employed to generate a modulation frequency of 2.5 kHz, which corresponds to the pulse on/off period of $\sim 400\ \mu s$ which is much larger than baseline ringdown time (RDT), $\tau_0 \sim 230\ ns$. A combination of a linear polarizer (HO-LFPS-25, Holmarc Opto-Mechatronics Ltd.) and a quarter wave plate (HO-WMQ-25M-633, Holmarc Opto-Mechatronics Ltd.) produced circular polarization of laser beam as well as obstruct back reflection into the laser cavity. A right-angled prism (PS908L- N-BK7, AR 350 – 700 nm, L = 20 mm, Thorlabs) was placed at the centre of the optical cavity, as shown in Fig. 1. The incident angle on the base of the prism was $\sim 72.84^o$, sufficient to satisfy the total internal reflection (TIR) condition for the current glass–water interface ($\theta_{Critical} \approx 61.4^o$), generating an evanescent wave on the base. A fast response photomultiplier tube (PMT) (R4632, rise time $\sim 2.2\ ns$, Hamamatsu) in combination with an amplifier unit (C9663, current-to-voltage conversion factor $\sim 4\ mV/\mu A$, Hamamatsu) was placed below the prism (see Fig. 1) to collect the ring-down signal with a high signal-to-noise ratio (SNR). A high-speed data acquisition card (100 MHz Bandwidth, 100 MS/s, 14-bit PCI-5122 Oscilloscope Device, National Instruments) was used to collect the data for ring-down events using a custom-made LabVIEW 2015 (64-bit) code (National Instruments). Fig. S1(b) and S1(c) show the variation of the ring-down time (RDT, τ_0) with the modulation frequency and the laser pulse's duty cycle. In the present experimental setup, we fixed the modulation frequency at $2.5\ kHz$ and the duty cycle at 65%

(~ 58.5 mW of laser power), optimizing τ_0 and the data's standard error (σ). The inset of Fig. S1(b) shows the variation of the ratio of RDT and σ with the laser's modulation frequency. It shows that the value of RDT/σ remains almost constant after 2.5 kHz. To estimate the optimized duty cycle of the laser pulse for the experiment, the variation of the RDT/σ with the duty cycle is plotted in Fig. S1(d). This figure estimates the optimized duty cycle for good RDT with minimum σ. The baseline RDT (τ_0) was estimated by placing water on the surface of the prism, keeping the laser's modulation frequency and duty cycle of 2.5 kHz and 65%, respectively. The distribution of the baseline RDT for 80 numbers of the averaging cycle is provided in Fig. S1(e). The Gaussian fit ensures that the EW-CRDS setup can effectively assess the concentration-dependent extinction without any significant drift in the mean τ_0. The average baseline RDT of $\tau_0 = 230\ ns$ for an empty cavity was attained with a standard error of 0.85% on averaging 80 ring-down events corresponding to an optical path length of $c\tau_0 \sim 69\ m$ and $c\tau_0/L \sim 51$ passes of light inside the optical cavity. Fig. S1(f) shows the Allan variance to estimate the stability of the cavity, and reaching an optimum integration time at $86^0\ s$.

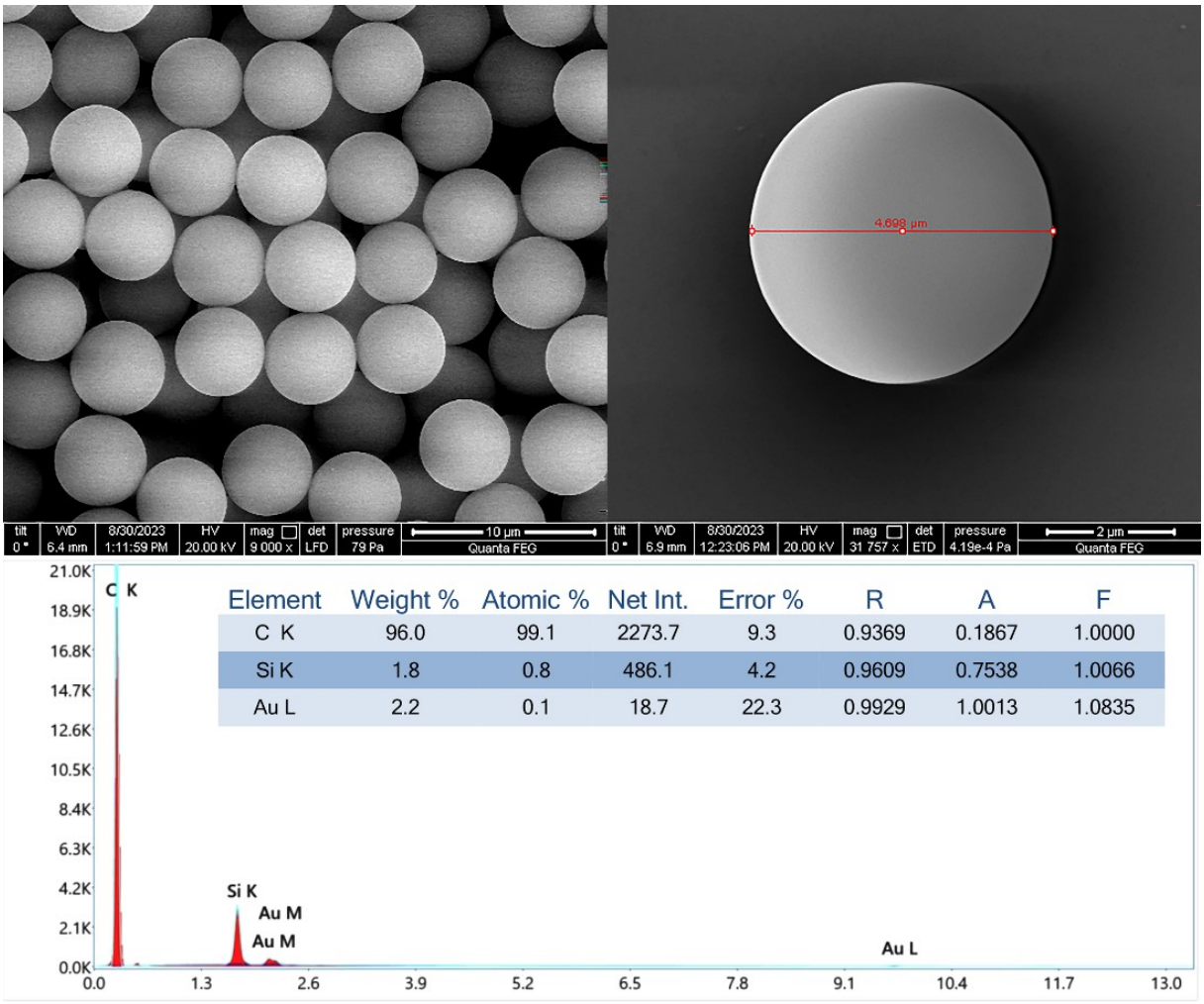

Element	Weight %	Atomic %	Net Int.	Error %	R	A	F
C K	96.0	99.1	2273.7	9.3	0.9369	0.1867	1.0000
Si K	1.8	0.8	486.1	4.2	0.9609	0.7538	1.0066
Au L	2.2	0.1	18.7	22.3	0.9929	1.0013	1.0835

Fig. S2 *SEM image of PSMs. It shows the uniform size of PSMs. The EDX spectra show that no impurities were there in the PSMs samples. Si and Au peaks are due to Si substrate and a thin layer of Au coating during the measurement, respectively.*

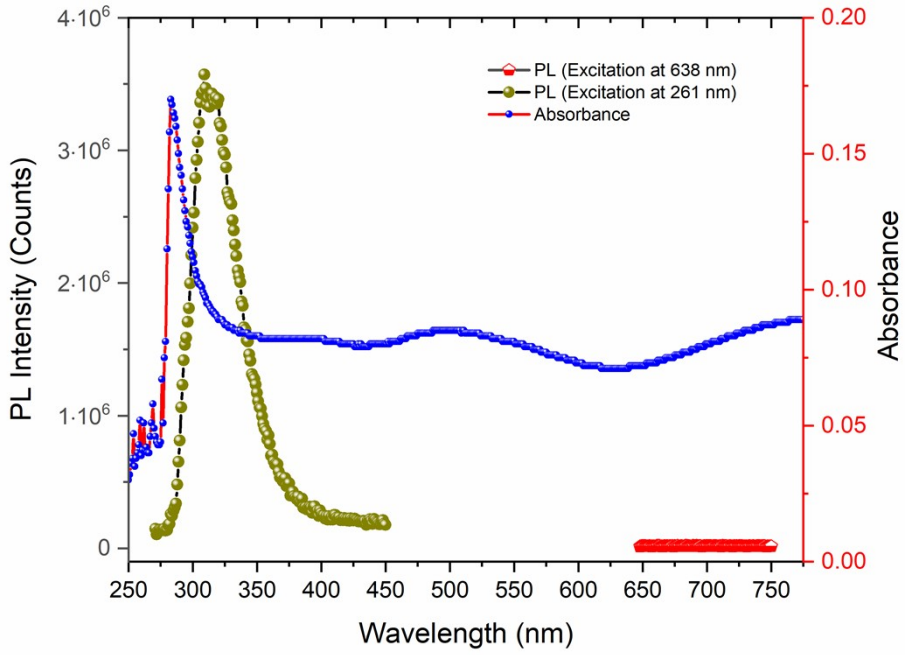

Fig. S3 *The figure shows the UV-Vis and Photoluminescence (PL) spectra of PSMs excited at 261 nm and 638 nm.*

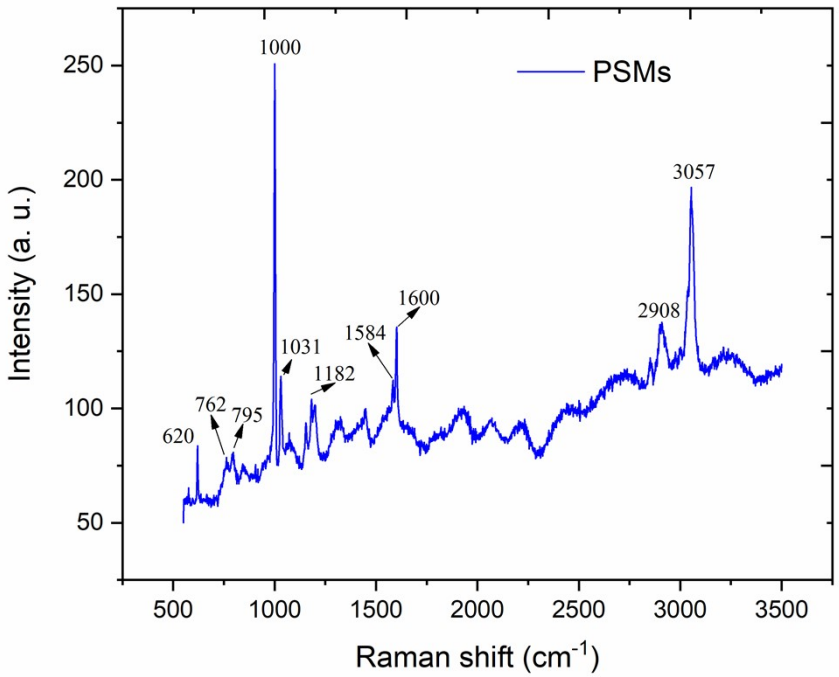

Fig. S4 Raman spectra for PSMs deposited on Si substrate.

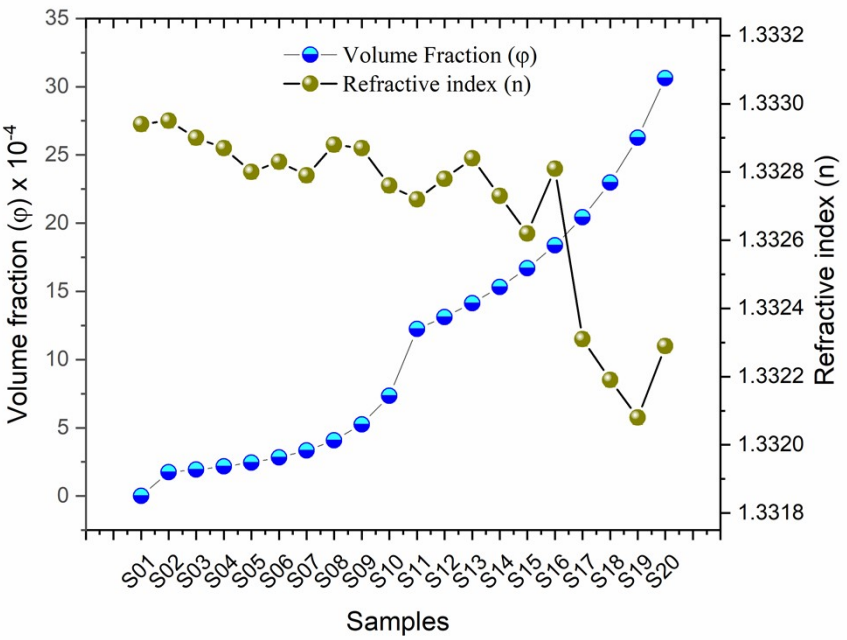

Fig. S5 The figure shows the variation of refractive index and volume fraction for various samples under study. However, the common refractive index measurement does not show much variation with volume fraction as the concentration of PSMs were very low to reflect in this data.

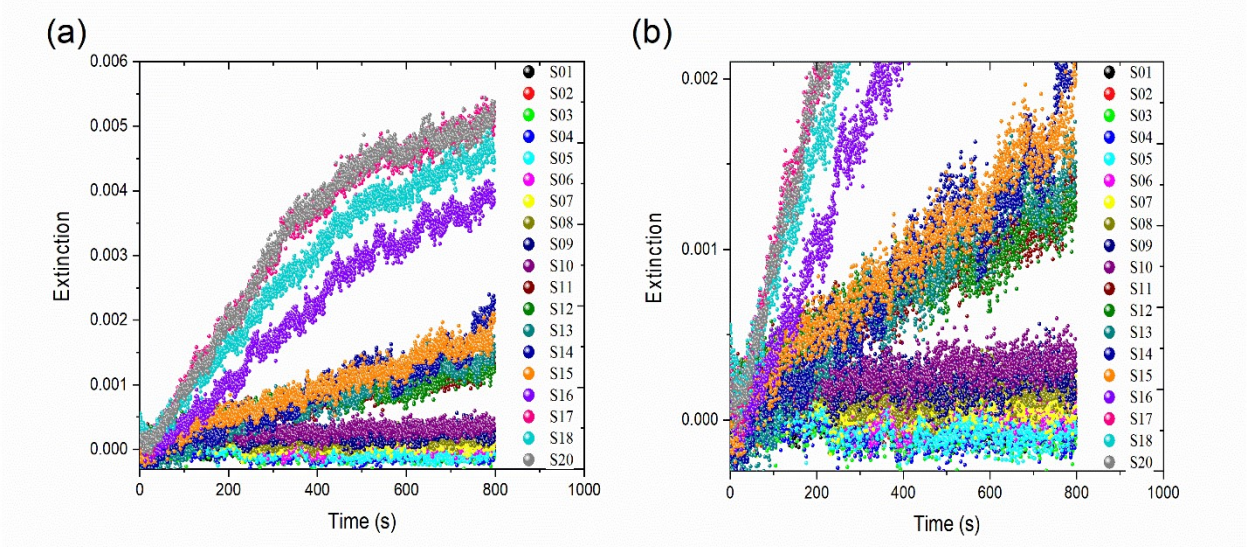

Fig. S6 (a) Change of extinction with time for all samples varying volume fractions of PSMs (S01 to S20). (b) The zoomed figure shows the slight variation of extinction with time for samples with lower volume fractions.